

Statistical Analysis of Competition Soaring

Christof Maul

Technische Universität Braunschweig, 38106 Braunschweig, Germany

Johann Wolfgang Goethe-Universität, 60487 Frankfurt, Germany

c.maul@tu-braunschweig.de

Abstract

Flight log data of three competition days of the Lüsse National Gliding Competition (Lilienthal Glide 2007) have been analyzed to extract vertical speed distributions and altitude distributions in space and time. Results are useful for forecasters and task-setters likewise. Analyzed dates were July 16, July 23, and July 26. These dates were chosen because they were characterized by a homogenous weather situation throughout the day, so that temporal evolution and spatial characteristics reflect pilot strategies rather than weather changes.

Nomenclature

h	altitude
t	time (UTC)
x	longitude
y	latitude
w	vertical speed
v	horizontal (air) speed
$f(h)$	altitude distribution
$f(w)$	vertical speed distribution
h_{in}	mean thermal entering altitude
h_{out}	mean thermal exiting altitude
h_{max}	maximum altitude
$f_{in}(h)$	thermal entering altitude distribution
$f_{out}(h)$	thermal exiting altitude distribution

Introduction

Establishing the use of satellite navigation-based flight data loggers has not only revolutionized soaring navigation and documentation, but also provides access to a huge set of data which can be employed in order to characterize meteorological conditions or pilots' tactical decision making.

The statistical analysis of individual flights is a standard de-briefing procedure for analyzing a pilot's performance. Systematic statistical analyses of ensembles of glider flights are less commonly found, notwithstanding previous use of instrumented birds for the investigation of the convective boundary layer^{1,2}. Previous work making use of a statistical approach includes the verification of thermal forecasts³ as well as several attempts to establish so-called "hot spot" databases and thermal strength analysis⁴⁻⁶. However, due to averaging over several days and large areas, the latter investigations might fail to recognize relevant features.

The motivation for the work presented here was to investigate the real behavior of competition pilots who optimize speed or flight distance under given conditions, as compared to the rather simplistic assumptions underlying speed-to-fly theory⁷. Main issues to be considered are 1) the distribution $f(h)$ of flight altitudes h and 2) the distribution $f(w)$ of vertical speeds w . As a matter of fact, speed-to-fly theory does not make assumptions with respect to the altitude band which is used by a pilot for cross-country flight other than finding a lift before hitting the ground. However, weather conditions, in the first place the wind vector, are not the same

for all altitudes. Therefore, the flight altitude will have an impact on the pilot's performance, even if the possible event of an outlanding is not considered. Secondly, speed-to-fly theory assumes a fixed average climb rate value as criterion for accepting a lift. Clearly, actual as well as lift-averaged climb rates used by a cross country pilot will considerably vary in the course of a flight.

Methods

In order to warrant identical conditions for the data to be analyzed, flight logs of the Lilienthal Glide 2007 were chosen for raw data. The competition was held in Lüsse near Berlin, Germany, from July 14 to 27, 2007, in three classes (15m, 18m, and Open) with altogether 97 competitors. All days were characterized by no to few outlandings and a high finishing rate. In total, 254 completed competition flights were considered in the analysis (for details refer to Table 1).

First, flight logs were cleaned from pre-start and post-finish data points. Then, in order to reduce the number of points without losing relevant information, the minimum time interval between adjacent data points was set to 24 seconds. This resulted in a set of altogether 126,904 data points (cf. Table 1), each of which is a vector consisting of five components: time t , latitude y , longitude x , altitude h , and vertical speed w . For the calculation of vertical speeds w the barometric altitude information was used instead of GPS-based altitude readings because GPS-based data contain numerous bad data points which would strongly affect climb and sink rates calculated from them. For obtaining a reasonably smooth result for the vertical speed distribution $f(w)$, it was necessary to average over two neighboring points.

Figure 1 shows the accumulated flight tracks $y(x)$ for all three competition days. The area shown is 11.8°E to 15.0°E and 51.1°N to 52.3°N. Lüsse airfield is marked by an open circle near the upper left corner of each diagram. For all three days, tasks for all classes covered a relatively small area (130 km by 220 km) which reaches into Polish territory on its eastern edge and which is limited by the air space C of metropolitan Berlin in the North and by the line Dresden-Leipzig-Halle-Magdeburg in the South and in the West. Figure 1 shows that the task area is densely and relatively homogeneously probed by the accumulated flight tracks. Due to the small size and the homogenous character of the

competition area, no attempt has been made to analyze the spatial variation of the flight log data.

Figure 2 shows accumulated variograms $w(t)$ for all three competition days. Except for the start and final glide phase, variation of vertical speeds is small throughout the race. The vertical speeds w shown here must not be confused with the meteorological movement of the air due to sink rate and stick lift effects.

First, vertical speeds w describe the actual vertical movement of the glider, not the updraft or downdraft of the air it flies in. Thus, the calculated vertical speeds w are lower than the meteorological values by the sink rate of the circling glider. In particular, the climb rates will be smaller than the updraft by the rate of least sink of the glider, and the calculated sink rates will reflect the (horizontal) air speed v of the glider rather than any vertical speed of the air itself (provided pilots prefer to minimize the time they spend in sinking air). Second, vertical speeds w are not corrected for changes in horizontal speed v , i.e. values in Fig. 2 (and in the analysis of the Vertical Speed section) contain the full effect of stick lift. Large vertical speeds w (positive and negative) are almost certainly due to this effect and should not be given too much weight in the further analysis. Generally, the spread in vertical speeds w is slightly exaggerated towards positive as well as towards negative values. Nevertheless, the number of such artificial data points is small. Consider, for example, a typical change in horizontal speed upon entering a thermal from $v_1 = 50$ m/s to $v_2 = 30$ m/s. The corresponding altitude gain is approximately 80 m, neglecting the effect of friction. If this altitude gain occurs within a single time interval of 24 s, the corresponding data point for the vertical speed w will be shifted up by 3.4 m/s whereas all following data points for the same thermal remain unaffected. If the altitude gained in a thermal by circling is assumed to be 600 m at an average climb rate of 2.5 m/s, there will be 10 data points showing correct vertical speeds for one data point affected by stick lift.

A correction of the data set for these two effects was not performed due to the heterogeneity of the data that have been obtained from 97 individual combinations of gliders and flight recorders. While glider polars are normally available, information on weight and ballast is normally missing, so the glider sink rate could be, at best, estimated roughly. More important, the elimination of both effects would require the determination of horizontal air speed and its changes, whereas flight recorders sample ground speed data. Conversion of one into the other would require wind data which are not readily available. Additionally, the determination of changes in horizontal speed require a high sampling rate of the flight recorder in order to precisely monitor direction changes made by the pilot, in particular while circling. However, minimum sampling rates in gliding competitions are too small to allow for a clear separation between speed and direction changes. The extraction of meteorological updraft from flight recorder data, therefore, would be feasible only in a well-controlled environment.

Figure 3 shows accumulated barograms $h(t)$ for all three competition days. Variation of altitude bands with time is more pronounced than the variation of vertical speeds.

Maximum altitudes and their variation with time are indicated in Fig. 3 by horizontal solid lines with 30 minute time resolution. Start and final glide phases have not been considered. July 16 is characterized by high flight altitudes close to the German legal altitude limit of FL100. Therefore, the July 16 altitudes reflect a legal barrier rather than a meteorological one and have consequently not been used for the altitude analysis.

Determining meteorologically meaningful maximum altitudes is not a straightforward task. The largest altitude in a given 30 minute interval or during a competition day is certainly not an appropriate value, in particular if a possible altitude gain in the order of 80 m by the variation of horizontal speed is considered. Therefore, the somewhat arbitrary value of the 99.75% percentile has been chosen as maximum altitude value h_{max} . This means that 99.75% of all data points have an altitude smaller than h_{max} . This value corresponds most closely to what one would determine as the maximum altitude intuitively, but at the same time allows the unbiased calculation of h_{max} .

Vertical speed

Two kinds of vertical speed distributions $f(w)$ are presented. The first has resulted from integrating over full competition days. The second one has been obtained with a 30 minute time resolution and allows one to follow the evolution of thermals and the flying strategy during the flight.

Time-integrated vertical speed distributions

Time-integrated vertical speed distributions $f(w)$ for each of the three days under consideration are shown in Fig. 4. Basically, they have been obtained by projecting the accumulated variograms $w(t)$ in Fig. 2 onto the w axis. Qualitatively, the distributions for all three days are identical. All are characterized by a bimodal distribution, clearly reflecting the two flight modes "climb" and "straight flight" (the latter will be termed "sink" from now on for reasons of brevity). Obviously conditions in this competition were such that pilots essentially obeyed the basic ideas underlying speed-to-fly theory and that aligned lift played only a minor role in pilots' decisions. Under different conditions which favor the occurrence of aligned lift, this bimodality is likely to be less pronounced or to vanish at all. While this is an interesting issue to be investigated, it is beyond the scope of the current article.

Climb and sink distributions have different integrated areas with sink dominating climb. This is less paradoxical than it might appear at first thought. First, the analysis comprises more sink than climb because the pre-start data have been eliminated from the analysis while final glide data have not. So every single flight has a net balance in favor of sink by the margin of the start altitude. Second, the integrated area is a measure for the number of data points used in the analysis, and the number of data points is related to the time spent in climb or sink. It can qualitatively be seen that the sink distribution peaks at a lower speed value than the climb distribution. Whereas the heights gained in climb and lost in sink must be the same except for the missing start altitude, the times spent in climb or sink are certainly not. An average climb rate that is

larger than the average sink rate implies that the time spent in sink is larger than the time spent in climb.

Figure 4 shows that the bimodal vertical speed distributions can be well described by sums of two Gaussian functions, one accounting for climb and the other one accounting for sink. The centers and widths of the distributions that have been returned as fit parameters are listed in Table 2. Strong climb correlates with larger sink, as a consequence of larger flying speeds. The widths of the distributions are almost the same for climb and sink distributions and are almost independent of the average climb speed.

Time-resolved vertical speed distributions

Time-resolved vertical speed distributions have been obtained for all three days by binning the complete set of data points into time intervals of 30 minutes width. Figure 5 shows the time-resolved vertical speed distribution for July 16. Time runs from the bottom to the top. In contrast to the integrated vertical speed distribution, here every trace is obtained by vertically slicing the cumulated variograms of Fig. 2. The analyses of the other two competition days are not shown here as they yield similar results. The general behavior of the distributions remains unchanged, with the centers of the distributions moving to larger values in the middle of the competition day and the last trace essentially being characterized by the final glide.

As was done for the integrated data, every 30 minute interval was fitted by a superposition of two Gaussian functions describing climb and sink distribution. Other than for the altitude distributions, meaningful results are obtained for the whole race, from start to final glide, since pilots will try to optimize their climb rate independently of tactical considerations or competition rules. A summary of the temporal evolution of the most probable climb and sink speeds at 30 minute time resolution is shown in Fig. 6. Additionally, Fig. 6 contains the average climb and sink rates listed in Table 2.

Altitude distributions

Time-integrated and time-resolved altitude distributions $f(h)$ were extracted from the flight logs as projections and slices of the cumulated barograms $h(t)$ of Fig. 3, similarly to the vertical speed distribution case in the Vertical speed section.

Time-integrated and time-resolved altitude distributions

Figure 7 shows three time-integrated altitude distributions for each of the three days under consideration: the climb altitude distribution, the sink altitude distribution, and the total altitude distribution which is the sum of the former two. Sink altitude distributions have slightly larger areas than climb altitude distributions for the reasons outlined in the Time-integrated vertical speed distributions section. The main differences occur at small altitudes and reflect the final glide parts of the flights. Apart from that, climb and sink altitude distributions are essentially identical implying that altitude averaged vertical speed is uncorrelated to altitude. Indeed, altitude averaged climb and sink values are essentially

independent of altitude as shown in Fig. 8. Altitude averaged vertical speeds determine altitude distributions and must not be confused with maximum values which do show a pronounced dependence on altitude. Maximum and minimum values have no effect on altitude distributions.

All altitude distributions are singly peaked, but their shapes are not Gaussian. Climb altitude distributions can be well described assuming two Gaussian distributions for thermal entering and exiting altitudes, as is in detail described in the sub-section below on 'Thermal entering and exiting altitudes - Methods'.

Figure 9 shows the evolution of the total altitude distribution over the competition day for July 26 with a 30 minute time resolution. Starting at the bottom, one observes an increase of mean and maximum altitudes together with a slight broadening of the distribution in the course of the day. The last (top) three traces indicate the transition to the final glide regime by the "leak-out" of the altitude distributions towards smaller values at the left.

Thermal entering and exiting altitudes - Methods

Distributions of thermal entering and exiting altitudes can be obtained by two substantially different methods, lift-based and differential, which will be described in more detail below.

The lift-based method uses direct determination of thermal entering and exiting altitudes relying on the identification of circling in thermal lift. For identification of a thermal the following criteria were used. First, the vertical speed w must be positive: $dh/dt > 0$. Second, ground speed must be small: $dx/dt \approx dy/dt \approx 0$, or combined in one condition: $(dx/dh)^2 + (dy/dh)^2 \approx 0$. If these conditions were met for at least four consecutive data points, it was assumed that the glider had entered thermal lift, and the altitude of the first data point satisfying all aforementioned conditions was taken to be the thermal entering altitude. Similarly, thermal exiting altitudes were determined.

The differential method uses indirect determination of thermal entering and exiting altitudes relying on the shape analysis of climb altitude distributions. Basically, thermal entering and exiting distributions are obtained by differentiating the climb altitude distribution with respect to altitude. Likewise, the climb altitude distribution can be obtained by integrating thermal entering and exiting altitude distributions.

While the lift-based approach can be applied in a straightforward way, the basis version of the differential approach outlined below requires making the following approximations. First, assume the climb rate to be constant within a thermal. Second, assume that for the analyzed period which can be a complete flight or any part thereof, the climb rate will be the same and constant for all thermals encountered. Thus, inside all analyzed thermals the same constant average climb rate of the period under consideration will be encountered, which is given by the center of the corresponding Gaussian vertical speed distribution $f(w)$.

Given the conditions described above, mathematically the altitude distribution $f(h)$ is given by the integral

$$f(h) = \int_0^h (f_{in}(h') - f_{out}(h')) dh' \quad (1)$$

where $f_{in}(h)$ and $f_{out}(h)$ are the distributions of entering and exiting altitudes. Then, these distributions can be extracted from a known in-flight altitude distribution $f(h)$ which can easily be obtained from the analysis of flight data logs. Determining $f_{in}(h)$ and $f_{out}(h)$ only requires taking the derivative of the in-flight altitude distribution $f(h)$.

$$\frac{df(h)}{dh} = f_{in}(h) - f_{out}(h) \quad (2)$$

Thermal entering and exiting altitudes - Results

Both methods, direct, lift-based and indirect, differential determination of thermal entering and exiting altitudes were performed for all three competition days. In the differential method, the integrated altitude distributions obtained by the procedure in the sub-section 'Time-integrated and time-resolved altitude distributions' were differentiated, and the resulting bimodal derivative was fitted by a sum of two Gaussian functions representing thermal entering and exiting altitude distributions. In the direct method, thermal entering and exiting distribution were determined from identifying thermal lift as described in the sub-section 'Thermal entering and exiting altitudes - Methods', and both distributions were fitted by Gaussian functions. The sum of the two Gaussian functions was integrated to obtain a calculated climb altitude distribution. Results of this procedure are given in Table 3 and in Figure 10.

It can be seen that the agreement of both methods with each other is excellent. Table 3 shows that, clearly, the direct, lift-based method results in much more precise values than the indirect, differential method relying on differentiating the climb altitude distribution. Nevertheless, centers and widths of thermal entering and exiting altitude distributions are reproduced within the error margins of the fitting procedure.

Figure 10 impressively demonstrates the excellent agreement of both methods with each other. In the lower panel, the July 23 climb altitude distribution synthesized from integrating lift-based thermal entering and exiting altitudes is compared to the climb altitude distribution directly obtained from the flight log data. Here, the lift-based analysis is used as an indirect method for determining altitude distributions. In the top panel of Fig. 10 the complementary information is shown. Thermal entering and exiting altitude distributions directly obtained with the lift-based approach are compared to the corresponding distributions indirectly obtained with the differential approach. In this case, the differential method is the indirect one. In both cases the agreement is excellent. Similarly, excellent agreement is also obtained for July 16 and July 26.

This excellent agreement shows that the assumptions of constant vertical speeds within and between thermals were fulfilled for all three competition days under analysis. Thus, the agreement proves that all three days can be satisfactorily

described by speed-to-fly theory. Therefore, the Lüsse competition should be regarded as a benchmark for the case of a pure speed-to-fly competition, i.e. a competition throughout which speed-to-fly theory was applicable. Conditions differing from speed-to-fly-theory conditions should easily be recognized from less good agreement or even complete disagreement of the lift-based and the differential methods for the determination of thermal entering and exiting altitude distributions.

The most relevant factors contributing to such deviations are expected to be 1) the existence of aligned lift and 2) a $w(h)$ correlation between (average) vertical speed and altitude. Aligned lift is not accounted for in direct determination of thermal entering and exiting altitudes, whereas in the indirect method it is dealt with as if it were a thermal with average climb vertical speed. A non-vanishing $w(h)$ correlation could be accounted for in principle by introducing altitude dependant weight factors to f_{in} and f_{out} distributions in equations (1) and (2). Such deviations are expected to occur for competition flights in structured terrain. The investigation of structured terrain competitions is in progress, and results will be published in a forthcoming paper.

In Table 4, the time dependence of thermal entering altitudes h_{in} , thermal exiting altitudes h_{out} , and their distribution widths are compared to the maximum altitudes h_{max} for July 23 and July 26. Direct, lift-based determination of thermal entering and exiting altitudes was used.

For July 16, no such analysis was performed because the maximum altitude was limited by legal regulations rather than by meteorological or flight tactical considerations. Likewise, a time-resolved analysis was performed only if start or final glide phases did not strongly affect the altitude distributions (cf. Fig. 3).

One obtains the following results: 1) The altitude band actually used for flying is relatively narrow; it covers between 20% and 30% of the maximum altitude. 2) The thermal exiting altitude lies between 75% and 85% of the maximum altitude. 3) In agreement with the previous two statements, thermal entering altitudes range from 50% to 65% of the maximum altitude. For identifying correlations between thermal entering and exiting altitudes and their distribution parameters with maximum altitudes or vertical speed values, more data need to be analyzed. For the time being, the data presented here suggest that such correlations do exist.

Conclusions

It has been demonstrated that a statistic analysis of flight log data is a valuable source of information for pilots, forecasters, and meteorologists. Although any such analysis never directly reflects the meteorological situation, but always includes the - generally unknown - pilot's and sailplane's response to the meteorological situation, the huge data set available and the density and global availability of such data make them a most useful tool for characterizing cross-country flying meteorologically as well as tactically.

Vertical speed distributions in unstructured landscape are bimodal and can be well described by the sum of two Gaussian functions, one centered at positive values (climb)

characterizing lift and one centered at negative values characterizing straight flight (sink). Variation throughout the race time is generally small.

Altitude distributions are singly peaked and generally asymmetric. They can be well described by integrating two Gaussian distributions, characterizing thermal entering and exiting altitudes. The variation of the altitude distributions during the race is more pronounced than the variation of vertical speed distributions. The altitude bands used are relatively narrow and account for about 25% of the thickness of the convective boundary layer. Generally, cross-country flying under the conditions of the Lüsse competition took place between 60% and 85% of the maximum altitudes, with lower and upper limits varying during the race.

Two methods have been presented for the determination of thermal entering and exiting altitude distributions, one relying on identifying the beginning and ending of circling in thermals, the second using mathematical manipulation of climb altitude distributions. Both methods are equivalent if standard speed-to-fly theory conditions are met. It has been shown that this was the case for all three Lüsse competition days under analysis. It is therefore suggested to regard the Lüsse competition as a benchmark speed-to-fly-theory competition. The equivalence of both methods demonstrated in this work will help to identify relevant deviation from standard speed-to-fly theory conditions.

Results are expected to be significantly different for other conditions, in particular in structured (mountainous) terrain,

under conditions of aligned convection, or for inhomogeneous weather situations.

Acknowledgments

Helpful discussions and critical reading of the manuscript by Olivier Liechti and Raluca Niesner are gratefully acknowledged.

References

- ¹Shannon, H., Young, G., Yates, M., Fuller, M. and Seegar, W., "Measurements of thermal updraft intensity over complex terrain using American white pelicans and a simple boundary layer forecast model", *Boundary Layer Meteorology*, 104, 2002, pp. 167-199.
- ²Shannon, H., Young, G., Yates, M., Fuller, M. and Seegar, W., "American white pelican soaring flight times and altitudes relative to changes in thermal depth and intensity", *The Condor*, 104, 2002, pp. 679-683.
- ³Liechti, O., Lorenzen, E., Thehos, R., Olofsson, B. and Olsson, E., "Verification of Thermal Forecasts with Glider Flight Data", *Technical Soaring*, 31, 2007, pp. 42-51.
- ⁴Termikanalyse, <http://www.pfg.dk/termikanalyse/>.
- ⁵Haas, T. and Maul, C., "Aufwinde nach Katalog - Thermikkarten neu gemischt", *Aerokurier*, 10, 2003.
- ⁶Ultsch, A., "Kurbeln oder weiterfliegen?", *Magazin Segelfliegen*, 1/2, 2005/1-2, pp. 14-18.
- ⁷Reichmann, H., *Streckensegelflug*, Motorbuch Verlag, 4th ed., 1979, pp. 146-179.

Table 1

Set tasks and number of analyzed flights.
Accumulated tracks are shown in Fig. 1. (SAA: speed area task).

day	number N of analyzed flights	number P of data points	class	task
16.07.	89	43283	open	441.5 km racing
			18m	374.9 km racing
			15m	348.0 km racing
23.07	78	39085	open	319.4 km racing
			18m	334.5 km racing
			15m	286.6 km racing
26.07.	87	44536	open	3:30 h SAA (283.1 km - 565.1 km)
			18m	365.4 km racing
			15m	356.9 km racing

Table 2

Results of fitting two Gaussian distributions to the vertical speed distributions of Fig. 4 (HWHM: half width at half maximum).

day	climb center, m/s	climb HWHM, m/s	sink center, m/s	sink HWHM, m/s
16.07.	2.15	1.14	-1.47	1.13
23.07.	1.40	0.99	-1.20	1.06
26.07.	1.56	1.06	-1.31	1.10

Table 3

Integrated thermal entering (f_{in}) and thermal exiting (f_{out}) altitude distributions. A: Results of fitting two Gaussian distributions to the derivative of the integrated climb altitude distributions from Fig. 7, based on Eq. 2. B: Results of fitting two Gaussian distributions to thermal entering and exiting altitude distributions directly determined from the flight log data. h_{in} and h_{out} are distribution centers. Maximum altitudes h_{max} were taken as 99.75 percentile of altitude data. (HWHM: half width at half maximum; $\Delta = h_{out}/h_{max} - h_{in}/h_{max}$)

day	h_{max} , m	f_{in}	f_{in}	f_{out}	f_{out}	h_{in}/h_{max}	h_{out}/h_{max}	Δ
		h_{in} , m	HWHM, m	h_{out} , m	HWHM, m			
16.07. A	2777	1409± 75	360±151	2307±492	774±762	50.7%	83.1%	32.4%
16.07. B		1469± 13	453± 20	2206± 28	550± 43	52.9%	79.4%	26.5%
23.07. A	1831	932± 49	240± 30	1368±113	324± 71	50.9%	74.7%	23.8%
23.07. B		950± 5	265± 6	1346± 7	288± 10	51.9%	73.5%	21.6%
26.07. A	1970	1184± 30	258± 30	1679± 17	198± 15	60.1%	85.2%	25.1%
26.07. B		1187± 6	281± 8	1625± 6	240± 7	60.3%	82.5%	22.2%

Table 4

Results of fitting two Gaussian distributions to integrated (bold face) and time-resolved (standard face) thermal entering and exiting altitude distributions directly determined from the flight log data. h_{in} and h_{out} are distribution centers. Maximum altitudes h_{max} were taken as 99.75 percentile of altitude data. (HWHM: half width at half maximum; $\Delta = h_{out}/h_{max} - h_{in}/h_{max}$)

day	h_{max} , m	f_{in}	f_{in}	f_{out}	f_{out}	h_{in}/h_{max}	h_{out}/h_{max}	Δ
		h_{in} , m	HWHM, m	h_{out} , m	HWHM, m			
23.07.	1831	950± 5	265± 6	1346± 7	288±10	51.9%	73.5%	21.6%
10.30-11.00	1531	907± 7	160± 8	1260± 7	197± 8	59.2%	82.3%	23.1%
11.00-11.30	1654	837±10	229±11	1327±27	265±31	50.6%	80.2%	29.6%
11.30-12.00	1769	1001±19	305±23	1403±16	261±19	56.6%	79.3%	22.7%
12.00-12.30	1895	1077±13	233±15	1506±27	340±32	56.8%	79.5%	22.7%
12.30-13.00	1779	1016±12	241±14	1364±16	278±19	57.1%	76.7%	19.6%
13.00-13.30	1809	969±11	266±13	1337±12	255±14	53.6%	73.9%	20.3%
26.07.	1970	1187± 6	281± 8	1625± 6	240± 7	60.3%	82.5%	22.2%
12.00-12.30	1752	1093±12	204±15	1536±19	235±22	62.4%	87.7%	25.3%
12.30-13.00	1787	1112±12	224±15	1518± 8	200± 9	62.2%	84.9%	22.7%
13.00-13.30	1847	1114±13	278±16	1607±15	247±18	60.3%	87.0%	26.7%
13.30-14.00	1992	1132±23	310±26	1649±13	234±15	56.8%	82.8%	26.0%
14.00-14.30	2020	1317± 8	209±10	1762± 9	219±11	65.2%	87.2%	22.0%
14.30-15.00	2000	1301±20	266±23	1671±11	195±13	65.1%	83.6%	18.5%

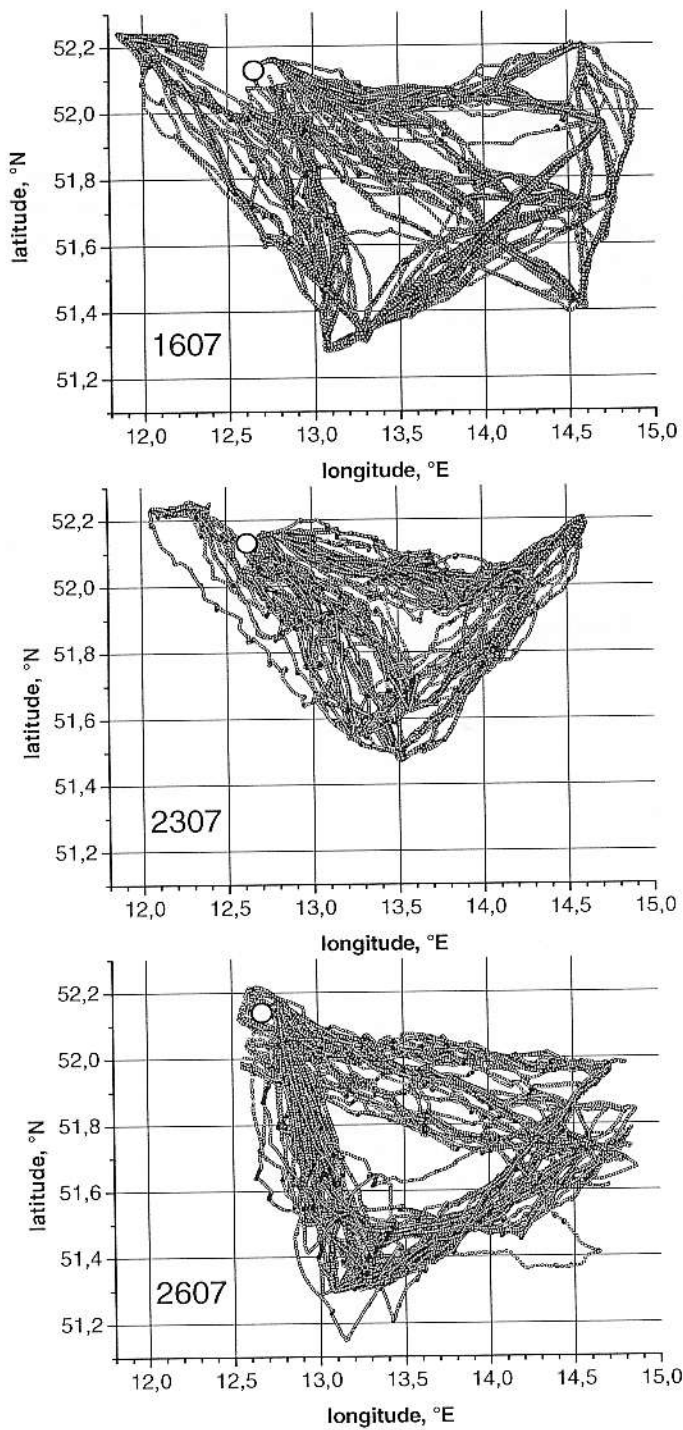


Figure 1 Accumulated tracks for all 254 analyzed flights. Lüsse airfield is marked by the open circle near the upper left corner.

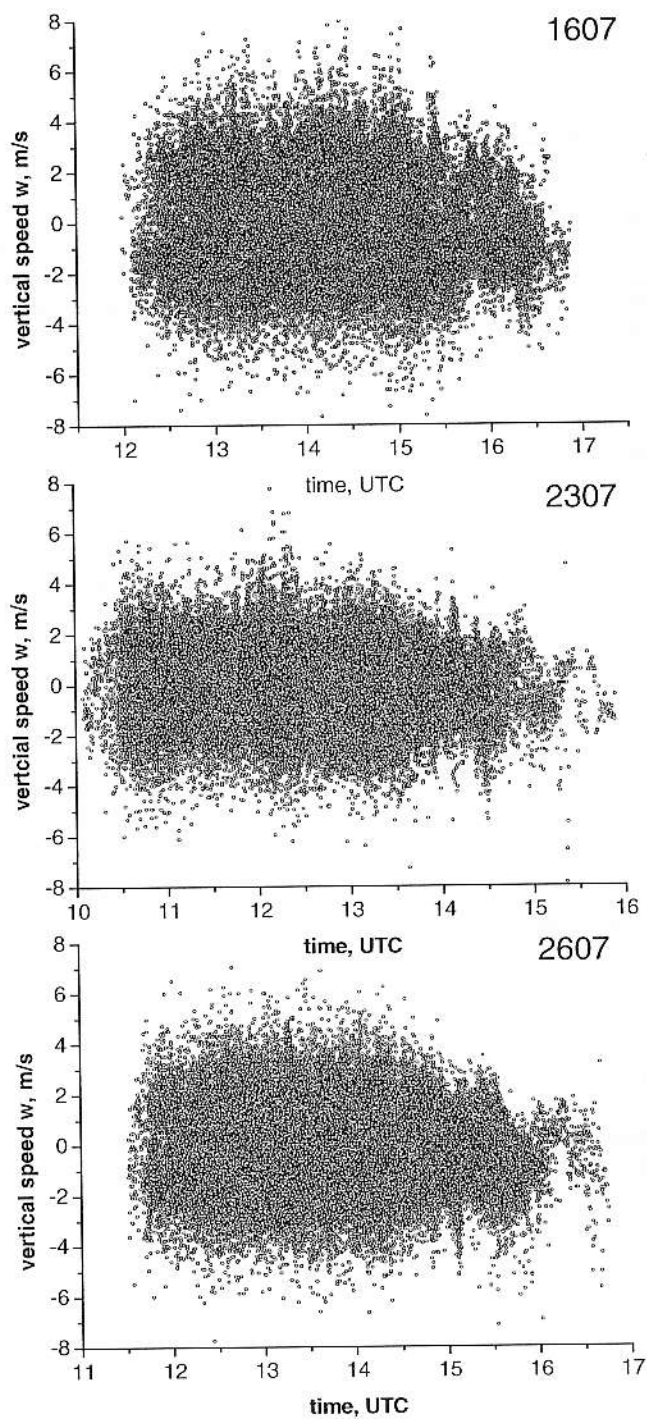


Figure 2 Accumulated variograms for all 254 analyzed flights.

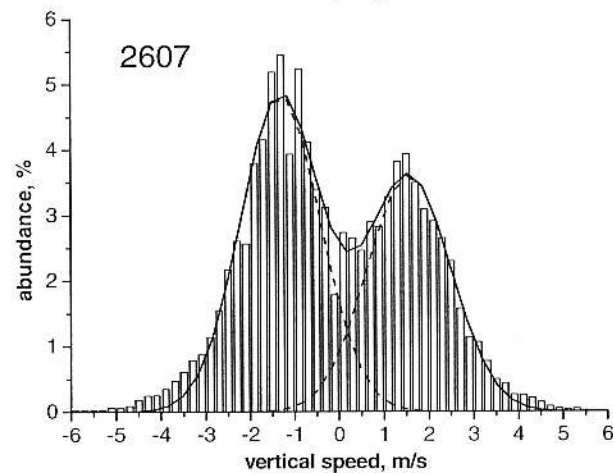
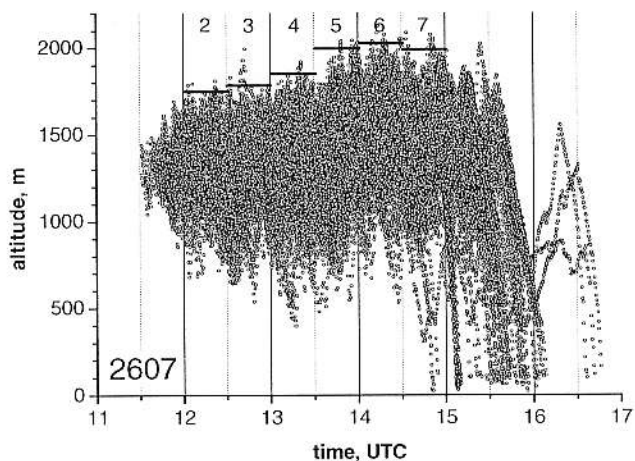
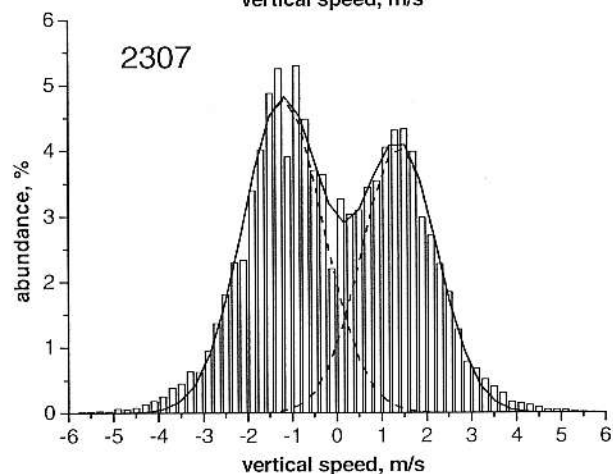
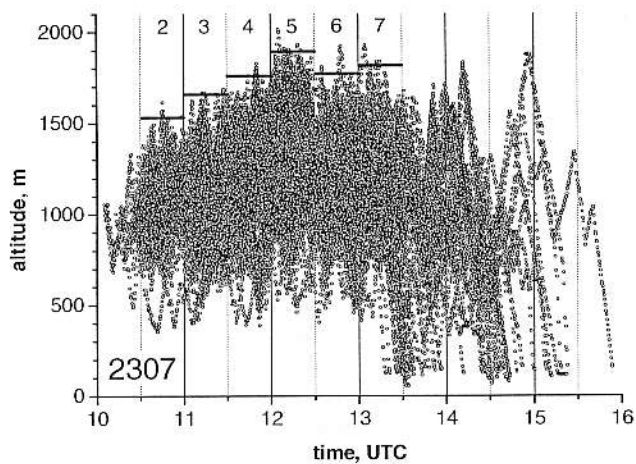
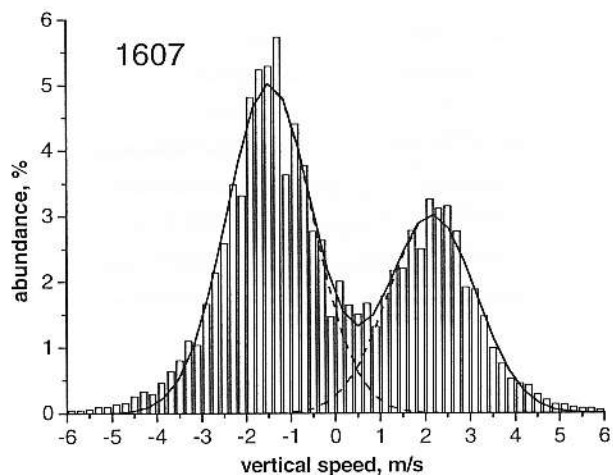
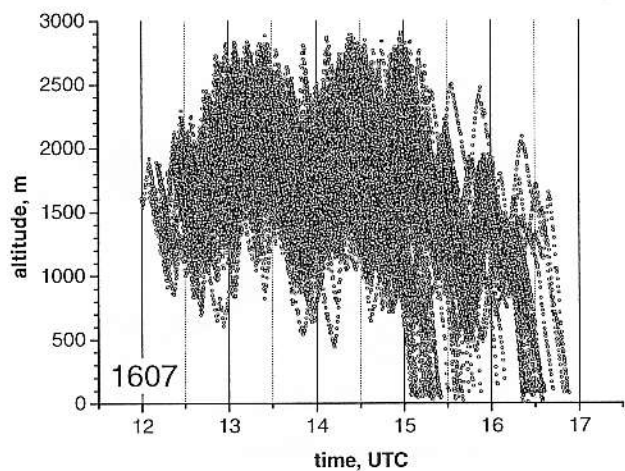


Figure 3 Accumulated barograms for all 254 analyzed flights. For July 16, the flat top between 13 and 15 UTC suggests maximum altitudes above 3000m which underlie legal restrictions. For July 23 and 26, maximum altitudes h_{max} are indicated by solid lines for 30 minute intervals, except for start and final glide phases. Time intervals are numbered where appropriate.

Figure 4 Normalized vertical speed distributions, integrated over whole competition days. The solid line is the best fit of two Gaussian distributions to the data. Dashed lines describe climb and sink distributions separately.

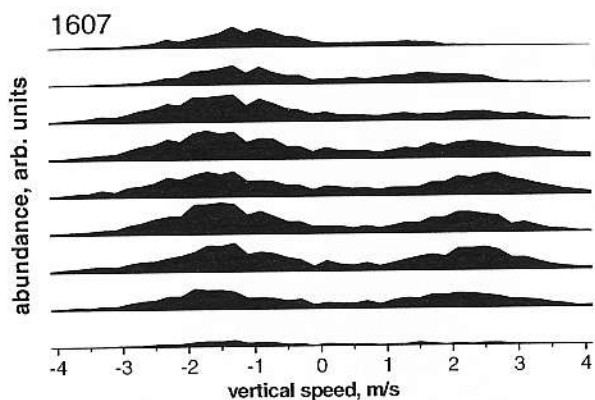


Figure 5 Time-resolved vertical speed distributions for July 16. The lowest trace is the first distribution after task start (1200 - 1230 UTC), the upper most trace is the last distribution before finishing (1600 - 1630 UTC). Time intervals have been set to 30 minutes. Distributions are not normalized, but reflect the actual number of racing gliders in each time interval.

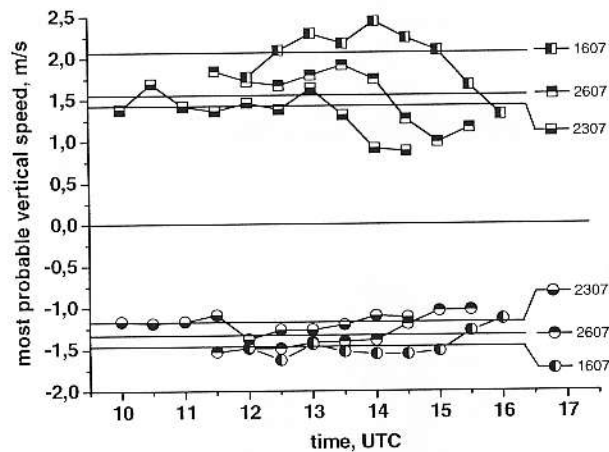


Figure 6 Temporal evolution of the most probable (climb and sink) vertical speeds for all three analyzed competition days with 30 minutes time resolution. Day averaged values are shown as straight lines.

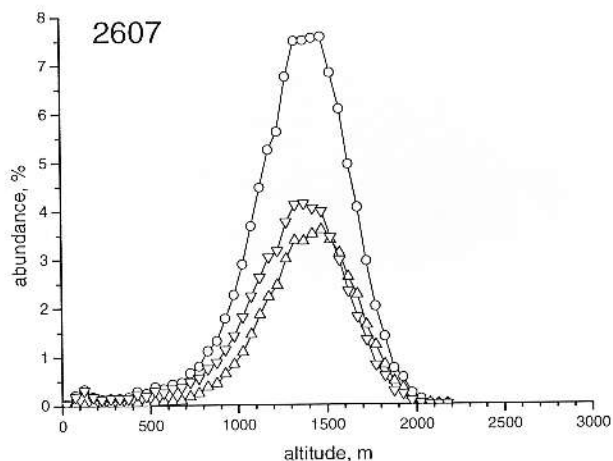
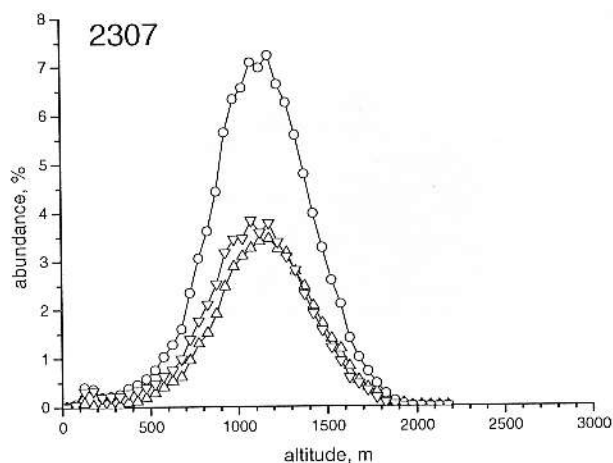
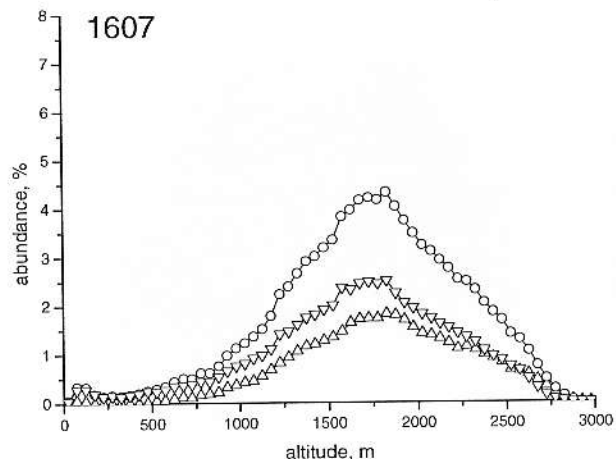


Figure 7 Total (circles), climb (upward triangles), and sink (downward triangles) altitude distributions. Larger amplitudes for sink than for climb reflect final glide phases. Apart from that, climb and sink distributions are essentially identical.

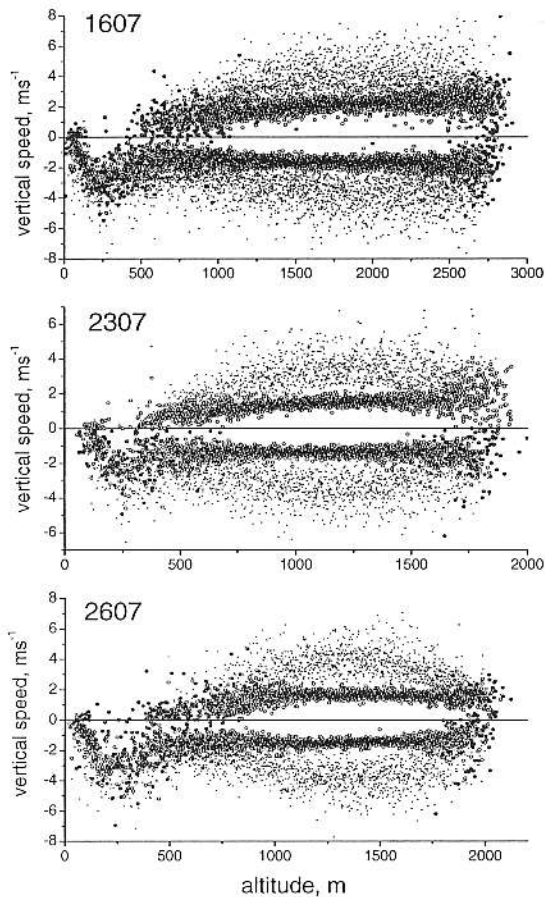


Figure 8 Altitude dependence of altitude averaged (large circles) and extreme (small circles) climb and sink values. Averaged values are essentially uncorrelated with altitude, whereas extreme values peak at medium altitudes.

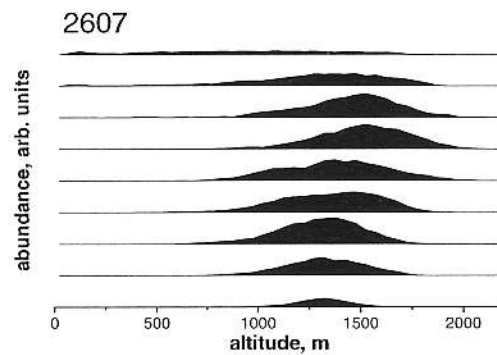


Figure 9 Time-resolved altitude distributions for July 26. The lowest trace is the first distribution after task start (1130 - 1200 UTC), the upper most trace is the last distribution before finishing (1530 - 1600 UTC). Time intervals have been set to 30 minutes. Distributions are not normalized, but reflect the actual number of racing gliders in each time interval.

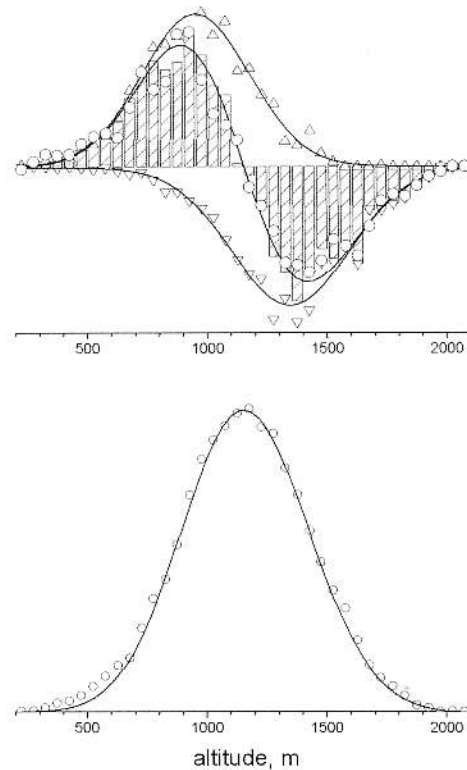


Figure 10 Upper panel: Thermal entering altitude $f(h_{in})$ (upward triangles) and exiting altitude $f(h_{out})$ (downward triangles) altitude distributions directly obtained from lift-based approach. Columns represent the combined data $f(h_{in}) - f(h_{out})$. Solid lines are Gaussian fits to individual and combined distributions. Open circles are $df(h)/dh$ values obtained from differentiating integrated altitude distributions. Lower panel: The solid line represents altitude distributions obtained from integrating the combined thermal entering and exiting distribution $f(h_{in}) - f(h_{out})$. Open circles represent the altitude distribution $f(h)$ directly obtained from analysis of flight log data.